Large-eddy simulation of a separated boundary layer

By W. Cabot

1. Motivation and objectives

In tests of wall models on a very coarse grid in the flow behind a backward-facing step (Cabot 1996), simple models in which wall stresses were modeled by assuming a local log law gave good results in attached regions but underpredicted the magnitude of the negative skin friction in the primary separated region, compared with well resolved large-eddy simulation (LES) results. More complicated thin boundary layer equations were able to give better overall results, but the negative skin friction predicted by this model was observed to be somewhat too large in magnitude. Because of the very coarse resolution, no model was able (or really expected) to capture secondary recirculation features in the corner. Subsequent tests (Cabot 1996, 1997) were ambiguous as to cause of this behavior, noting that the near-wall eddy viscosity model (a mixing length prescription with a wall damping function) was ill suited for separated flow and that the standard subgrid-scale (SGS) model used was inaccurate for coarsely gridded near-wall meshes. The severe corner geometry was also thought to be complicating the interpretation of the results. To provide a clearer test case for wall modeling in complex, separated flow without such geometrical complications, a new test case was chosen featuring mild separation on a flat plate due to an induced adverse pressure gradient, for which Na & Moin (1998) had performed a direct numerical simulation (DNS) at a low Reynolds number. The goal of recent work has been to perform a less expensive LES of this flow with a well resolved wall for use as a test case for evaluating the performance of wall models with coarsely resolved walls (Cabot 1997). Initially, the same low Reynolds number case as the DNS was to be simulated to validate the LES with well resolved walls and then used to perform tests of LES with coarsely resolved walls using wall models. Further, with the general shift to parallel supercomputing architectures and the diminishing availability of serial time, the separated boundary layer codes needed to be converted to a portable parallel framework (MPI) and validated with results from the extant serial vector code.

The status of the separated boundary layer simulations is given in §2 and the directions for future simulations and wall model tests therein are given in §3.

2. Accomplishments

The flow configuration for the separated boundary layer simulation is described in detail by Na & Moin (1998): A flow field from Spalart's (1988) DNS boundary layer simulation is perturbed and interpolated onto the inflow plane of flow over a flat plate. Strong sucking is introduced along the top zero-vorticity boundary followed by strong blowing, which induces a strong adverse pressure gradient in the

middle of the computational domain. The flow undergoes mild separation along the bottom wall, then partially recovers before it exits the domain using convective outflow boundary conditions. The Reynolds number at the inflow plane is about 300 based on momentum thickness and 500 based on displacement thickness $\delta^\star$. The computational domain is $357 \times 64 \times 50$ in units of $\delta^\star$ in the streamwise, wall-normal, and spanwise directions, respectively. The grid is uniform in the streamwise and spanwise directions and stretched with hyperbolic tangent profiles in the wall-normal direction.

2.1 Codes

Serial Code. The second-order staggered central finite difference serial code used by Na & Moin (1998) was modified to include the dynamic SGS model, both in its standard form (Germano *et al.* 1991, Lilly 1992) and in a "mixed" form (Zang *et al.* 1993, Vreman *et al.* 1994). In the former, the trace-free (*) part of residual stress is modeled as a purely dissipative term:

$$(\overline{\boldsymbol{u}\boldsymbol{u}} - \overline{\boldsymbol{u}}\,\overline{\boldsymbol{u}})^* \sim -2\nu_t \overline{\boldsymbol{S}} \,, \tag{1}$$

where $(\overline{\ })$ denotes the filter, ν_t is the eddy viscosity, and $\boldsymbol{S}$ is the strain tensor; in the latter, the model also includes a self-similar part:

$$(\overline{\boldsymbol{u}\boldsymbol{u}} - \overline{\boldsymbol{u}}\,\overline{\boldsymbol{u}})^* \sim (\overline{\overline{\boldsymbol{u}}\,\overline{\boldsymbol{u}}} - \overline{\overline{\boldsymbol{u}}}\,\overline{\overline{\boldsymbol{u}}})^* - 2\nu_t \overline{\boldsymbol{S}} \,. \tag{2}$$

Further, the option to use two forms of the eddy viscosity was implemented: either a "Smagorinsky" (1963) form,

$$\nu_t = C\overline{\Delta}^2 (2\overline{\boldsymbol{S}} : \overline{\boldsymbol{S}})^{1/2} \,, \tag{3}$$

where $\overline{\Delta}$ is the effective filter width, or a "Kolmogorov" form (Carati *et al.* 1995),

$$\nu_t = C\overline{\Delta}^{4/3} \varepsilon^{1/3} \,, \tag{4}$$

where the dissipation rate ε is assumed to be constant with filter width. In most runs the Kolmogorov form was used since it is less expensive to use with the dynamic procedure and gives very similar results compared with the Smagorinsky form; the Kolmogorov form was used for all of the results reported later in this section.

The serial LES code originally used second-order test filters and, in the case of the mixed model, second-order grid filters as well; these are of the form

$$\widehat{u} = u + (h^2/6)\delta^2 u \,, \tag{5}$$

where h is the filter half-width and δ^2 is the discrete second derivative. Second-order filters used with the standard dynamic procedure were found to generate large, spurious eddy viscosities in the regions below the vigorous top-wall transpiration, which often led to unstable growth of a spurious velocity signal there. This occurs because

the second-order filter produces residuals for low-order, large-scale variations in the mean flow that have nothing to do with turbulence. For example, if u in Eq. (5) has a linear variation in x, then $\widehat{uu} - \widehat{u}\widehat{u} = (h^2/6)(du/dx)^2$. The mixed model does not suffer as much from this defect, because residuals up to fourth order are treated by the self-similar term in the model, removing them from the dissipative term in the dynamic procedure. For tests with the standard dynamic procedure, it was necessary to implement fourth-order test filters (Vasilyev *et al.* 1998) of the form

$$\widehat{u} = u - (h^4/16)\delta^4 u \ , \tag{6}$$

which also greatly reduces spurious eddy viscosity generation although it is not necessarily consistent for use in second-order codes.

Parallel Code 1. The previous serial LES code was ported to a MPI version (with M. Fatica), which allows it to run on a variety of parallel machines with little modification. Along the way, the solver was updated to enforce continuity at each substep in the time advancement scheme rather than at the end of the full time step only, which increases the accuracy of the solver. Further, a bug was found (and corrected) in the original serial code's inflow interpolation scheme that was adding spurious noise to the inflow signal. The computational domain is chunked only in the wall-normal direction into planar slabs, which allows plane filtering to be performed in the standard dynamic procedure without any additional processor communication. The dynamic mixed SGS model has not been implemented in this version of the code. This parallel LES code has been run on a SGI Origin 2000 and Cray T3Es, and it has been validated by a detailed comparison with results from the serial code.

Parallel Code 2. A newer, faster LES boundary layer code has been supplied to us by C. Pierce (personal communication), which was written from the ground up in Fortran 90 and MPI, also using second-order finite differencing and a standard implementation of the dynamic procedure for the SGS model. One significant structural difference from the previous code is that the domain is chunked both in the wall-normal and streamwise directions for greater efficiency in communication. The appropriate boundary conditions for the separated boundary layer case have been implemented, as well as fourth-order test filtering for the dynamic procedure. The inflow conditions in this code are interpolated in a different way than in Na & Moin's (1998) code, which leads to some differences in the results; the issue of setting up consistent inflow conditions will be discussed later in more detail. This code is currently being tested on an Origin 2000 and will be ported to a T3E as well. Because Pierce's code is cleaner and appears to be appreciably faster than the parallel version based on Na & Moin's code, it will probably be used as the primary simulation code in future work.

2.2 Preliminary results

The LES test cases use the same domain size and boundary conditions as Na & Moin's (1998) DNS case except that inflow conditions are interpolated onto a coarser grid. Two LES grids were chosen: *Grid 1* resolves the viscous region along

the lower wall, using the same stretching as Na & Moin in the wall-normal direction with half as many grid points; *Grid 2* does not resolve the wall, using an even coarser, nearly uniform grid. (The grid cannot be coarsened very much near the top boundary without developing numerical instabilities in the laminar blowing region.) Grid 1 uses 7 times fewer computational cells than the DNS: $256 \times 108 \times 64$ computational cells in the streamwise, wall-normal, and spanwise directions, respectively, as compared to $512 \times 192 \times 128$ used in the DNS. The time step based on the CFL criterion is about 4 times greater for this LES case compared to the DNS. Grid 2 uses $160 \times 80 \times 48$ computational cells, or about 20 times fewer grid points than the DNS with time steps about 25 times greater. Near the inlet Grid 1 has about 10 points in the viscous sublayer ($y^+ < 10$) and 45 points in the whole boundary layer, while Grid 2 has about 10 points in the boundary layer with the viscous sublayer completely unresolved. Simulations were performed on these grids with and without the SGS model active to assess its effect. No wall model was used in these initial tests with Grid 2, such that the wall stress was generally much too low.

Grid 1. When no SGS model is active, the turbulence in the inlet section is more intense than in the DNS. Separation occurs later than in the DNS, and the near-wall pressure is too high in the separated region, as seen in Fig. 1 for the wall stress and pressure coefficient. When the SGS model is active, the major effect is a dramatic drop in the wall-normal and spanwise turbulence intensities in the inlet section, as illustrated in Fig. 2 for the wall-normal rms velocity at a height of about half of the inlet boundary thickness. The boundary layer thickens too rapidly upstream of separation, and separation tends to occur early, especially in the case using the dynamic mixed SGS model. The skin friction is seen to drop much too rapidly in the whole inlet section in Fig. 1. Visualizations confirm that the flow in fact undergoes partial relaminarization, then undergoes a transition of sorts back to a turbulent state just in front of the separated region. Reverse flow along the wall appears to travel quite far up the laminar patches ahead of the main separation bubble. This occurs for all SGS models, even though in the mean separation point for the standard dynamic SGS model case appears to be in good agreement with the DNS position.

Grid 2. The relaminarization of the inflow turbulence is less severe in the case with the unresolved wall although it still occurs to some extent. In Fig. 3 the near-wall streamwise velocity is shown in lieu of the wall stress, which cannot be determined reliably on the coarse wall-normal grid. Results for the standard dynamic SGS model are shown using Parallel Codes 1 and 2. Differences in results are seen in the inlet region due to different interpolation schemes of the inflow data (the former using spatial interpolation, the latter using spatial and temporal interpolation). The near-wall velocity stays in fair agreement with the DNS in the inlet region with Code 1 slightly slower and Code 2 showing some excess acceleration. At the outlet, the flow is much faster than in the DNS, which is expected, since the coarse grid cannot predict enough drag on the wall. The fair agreement of the near-wall flow speed in the inlet region is somewhat fortuitous, arising from a balance of

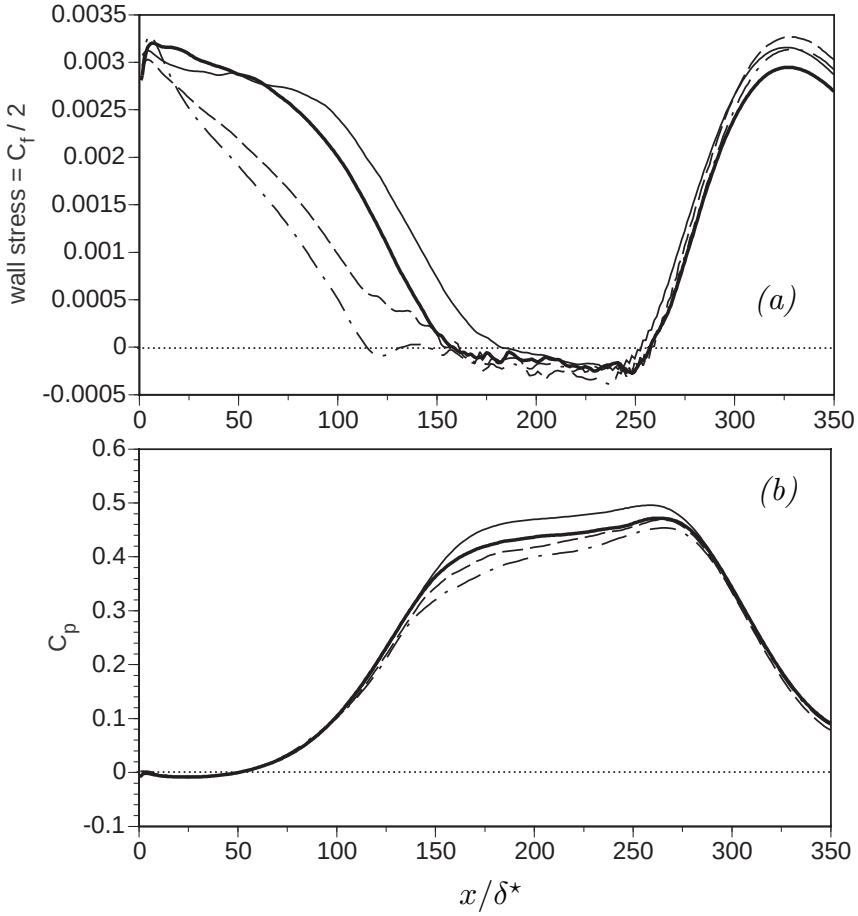

FIGURE 1. (a) The wall stress and (b) the pressure coefficient from the DNS and LES with a well resolved wall (Grid 1): ——— Na & Moin's (1998) DNS (serial code); ——— Grid 1 with no SGS model (serial code); - - - - LES with standard dynamic SGS model (parallel code 1); —— — LES with dynamic mixed SGS model (parallel code 2). The pressure coefficient is set relative to the pressure at $x/\delta^\star = 50$.

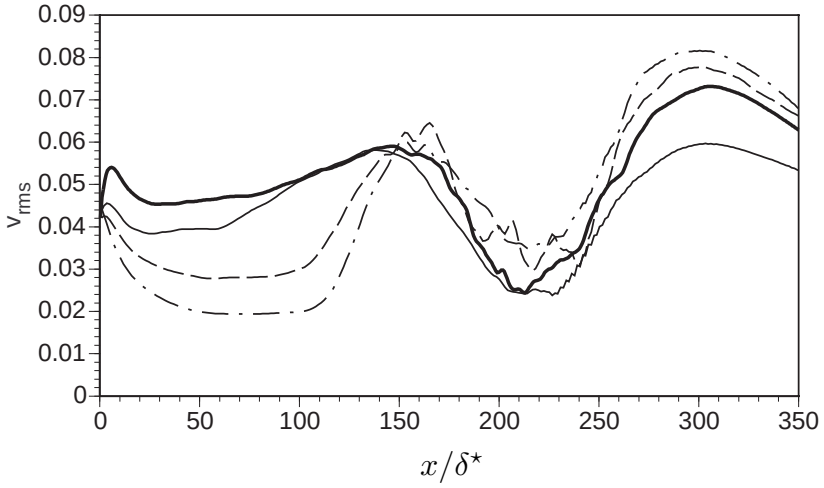

FIGURE 2. The wall-normal rms velocity from the DNS and LES with a well resolved wall (Grid 1) at a height $y = 2.9\delta^\star$: same symbols as in Fig. 1.

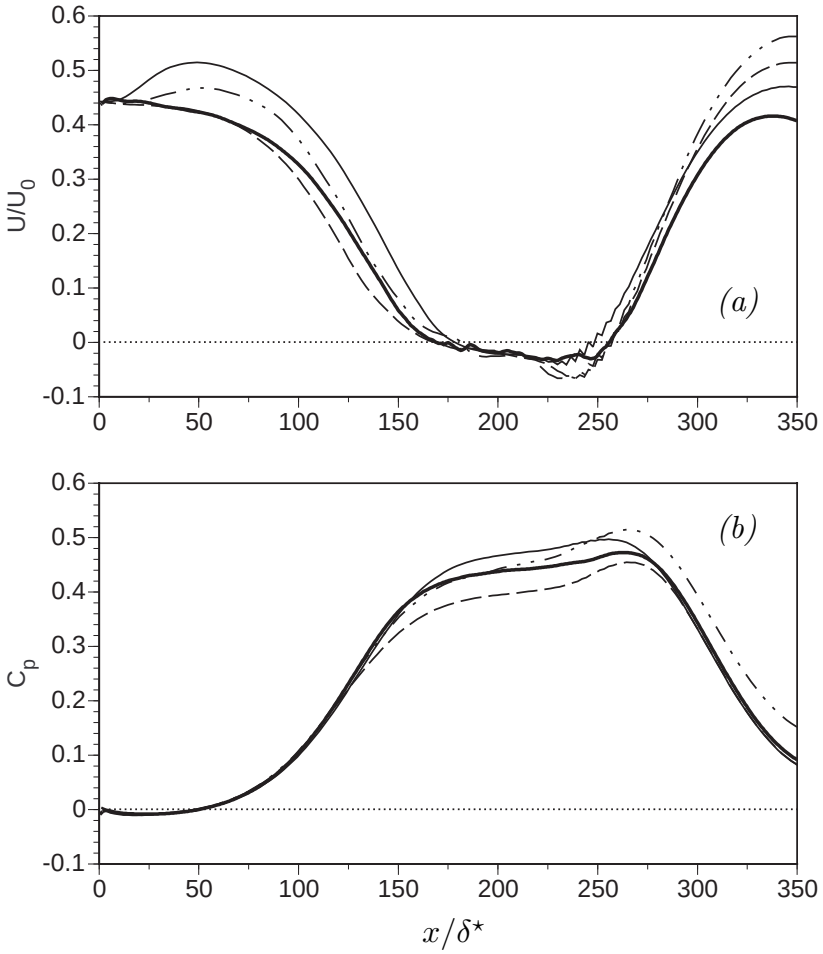

FIGURE 3. (a) The wall stress and (b) the pressure coefficient from the DNS and LES with an unresolved wall (Grid 2): ——— Na & Moin's (1998) DNS (serial code); ——— Grid 2 with no SGS model (parallel code 1); LES with standard dynamic SGS model using - - - - parallel code 1 and —·—·— parallel code 2. The pressure coefficient is set relative to the pressure at $x/\delta^\star = 50$.

too low drag with the opposing effect seen on Grid 1 due to the relaminarization of the inflow turbulence.

The reattachment point appears to be rather insensitive to the SGS model and grid, being set for the most part by the strong blowing peak from the top boundary. When no model is active, the reattachment occurs slightly early, while it occurs at the same location as in DNS when the SGS model is active. While mean flow quantities are not very sensitive to the SGS model downstream of reattachment, the turbulence intensities are much more sensitive, probably reflecting the very different upstream conditions that develop in the inlet region. With no SGS model, the turbulence intensities, that were comparable or higher than DNS values in the inlet region, are lower in the exit region. The reverse is true when an SGS model is active (cf. Fig. 2). Obviously more consistent inflow conditions need to be set up in the different cases to facilitate meaningful comparisons of overall flow statistics.

Calculated flow fields exhibit numerical oscillations for all grids, especially in the wall-normal velocity component near the reattachment point. These oscillations are especially pronounced in Grid 2, which may require some refinement in this region in future simulations to reduce this effect. It is not known if these oscillations are responsible for the pronounced peak near the reattachment point in near-wall velocity and pressure seen in Fig. 3 or if this is due to other factors such as the underprediction of wall stress or shear layer stress. Simulations with wall models will help answer this question.

3. Future plans

3.1 LES

The inflow generation technique described by Lund *et al.* (1998) will be used to provide consistent conditions at the inlet for the different separated boundary layer cases. In this scheme, the same numerical scheme, grid, time step, SGS model, and wall model to be used in the separated boundary layer simulation are used in a zero pressure gradient flat plate simulation in which the inflow data is generated by rescaling a plane in the flow near the outlet (but far enough away from the outlet not to be seriously contaminated by the convective outflow condition). After the inflow simulation has reached a statistical steady state, a history of the flow field at a plane in the middle of the numerical domain with the desired momentum thickness will be recorded and be used as the inlet boundary condition in the separated boundary layer simulation. Initial tests with this scheme successfully remove the strong transients in the inlet section evident with the old scheme. Because these new inflow conditions will necessarily differ to some extent from the original DNS by Na & Moin (1998), it may still be difficult to get a very quantitative comparison between LES and DNS.

In the first series of simulations with the new inflow conditions, the same Reynolds number as in the DNS will be used, mostly to validate the performance of the LES. The dynamic mixed SGS model will also be implemented in the parallel codes for comparison. Later it may prove useful to perform LES of the separated boundary layer with and without wall models at much higher Reynolds numbers, where both the SGS and the wall modeling are expected to perform better.

Wall models will be used to supply wall stresses to the LES with unresolved walls. The first set of tests will involve an approach like that used in simulations of flow over a backward-facing step (Cabot 1996). Solutions of simple ODEs or more expensive PDEs based on thin boundary layer equations are computed on a separate, refined near-wall grid and used to predict the wall stress when matched to outer LES flow conditions; the latter approach has been found to give reasonable mean values of wall stress even in separated regions where the equations are known to be invalid. We then intend to implement the more sophisticated v^2f RANS model (Durbin 1991) in the refined near-wall region. Ultimately we will blend it smoothly into the LES's SGS model throughout the near-wall region using a single grid refined in the wall-normal direction (Shur *et al.* 1998; also see discussion by Baggett in this volume). Also note that because the inflow generation calculations

must use the same wall models as the main calculation, this will also provide an additional test of wall modeling in a zero pressure gradient boundary layer.

3.2 Wall modeling issues

A number of outstanding issues concerning the proper way(s) of simulating near-wall regions remain to be resolved, and we will attempt to address many of these issues in future work.

As demonstrated by Baggett *et al.* (1997), a proper LES must resolve all the large energy-containing scales in the flow, which, however, become very small relative to outer scales near walls both in the wall-normal and tangential directions. An example of a proper (but more expensive) LES is that by Kravchenko & Moin (1998), which used a zonal mesh refined in all directions near the wall. It is more usual in LES of wall-bounded flow to use fine resolution only in the wall-normal direction near walls in conjunction with SGS model based on isotropy and self-similarity in the inertial range (usually modified with a wall damping function or the dynamic procedure to get the right asymptotic behavior); such models are not well suited for the near-wall region because the flow is highly anisotropic and the energy-containing scales in the horizontal directions are not resolved. The flow may be better described by a RANS solution near the walls, which is motivating the search for ways to meld RANS and LES descriptions in the near-wall region (cf. Baggett in this volume). Most RANS models still require special near-wall treatment in the form of wall damping functions. The wall's blocking effect is handled more physically in Durbin's (1991) $v^2 f$ model without the aid of damping functions, but the model is more complex, and it will be a challenge to incorporate it in LES. Another problem with most RANS models and thin boundary layer equations is that they rely on an eddy viscosity parameterization of the Reynolds stress, which is not valid in separated regions where turbulence and Reynolds stress is, to a large extent, convected rather than produced (Le *et al.* 1997). While this suggests that transport equations for Reynolds stresses are required, these are currently felt to be prohibitively expensive. Other options may prove to be more economical, e.g., resolving separated regions (since structures there are largely laminar, albeit small in scale), or applying special scaling or modeling relations in separated regions based on local flow criteria.

Although one can attempt to avoid simulating the near-wall region altogether by placing the numerical boundaries at off-wall locations, it is has proven very difficult to specify accurate enough boundary conditions to avoid generating spurious off-wall boundary layers and large pressure fluctuations (cf. Baggett 1997; Jiménez & Vasco 1998; Nicoud *et al.* 1998), and this approach will probably not be pursued in this flow.

On meshes (or more correctly, *for filters*) that are very coarse in the wall-normal direction near the wall, the issue of defining meaningful filters normal to the wall and consistent wall boundary conditions remains unsettled. This issue is skirted in LES with well resolved walls in which the filter is assumed to be comparable to the grid spacing, since filtering in the wall-normal direction near the wall has little effect. It would be worthwhile to consider performing LES and *a priori* DNS tests on

refined grids but with very broad near-wall filters in order to better understand the effects of near-wall filtering, in particular whether supplemental stresses need to be supplied only at the wall or, as we expect, throughout the boundary layer. Another closely related problem is defining consistent boundary conditions for the outer flow. Because there is no specific spatial information within a given filter width near the wall, one has virtually no wall information for filters much coarser than the viscous sublayer or the buffer region in a boundary layer, and hence both slip conditions and locally permeable conditions are admissible — and perhaps necessary for an accurate description.

Acknowledgments

Some of the simulations were performed on a Cray T3E at the University of Texas under a NPACI grant.

REFERENCES

Baggett, J. S. 1997 Some modeling requirements for wall models in large eddy simulation. *Annual Research Briefs 1997*, Center for Turbulence Research, NASA Ames/Stanford Univ., 123-134.

Baggett, J. S., Jiménez, J., & Kravchenko, A. G. 1997 Resolution requirements in large-eddy simulations of shear flows. *Annual Research Briefs 1997*, Center for Turbulence Research, NASA Ames/Stanford Univ., 51-66.

Cabot, W. 1996 Near-wall models in large eddy simulations of flow behind a backward-facing step. *Annual Research Briefs 1996*, Center for Turbulence Research, NASA Ames/Stanford Univ., 199-210.

Cabot, W. 1997 Wall models in large eddy simulation of separated flow. *Annual Research Briefs 1997*, Center for Turbulence Research, NASA Ames/Stanford Univ., 97-106.

Carati, D., Jansen, K., & Lund, T. 1995 A family of dynamic models for large-eddy simulation. *Annual Research Briefs 1995*, Center for Turbulence Research, NASA Ames/Stanford Univ., 35-40.

Durbin, P. A. 1991 Near wall turbulence closure modeling without "damping functions". *Theor. Comput. Fluid Dyn.* **3,** 1-13.

Germano, M., Piomelli, U., Moin, P., & Cabot, W. H. 1991 A dynamic subgrid-scale eddy viscosity model. *Phys. Fluids A* **3**, 1760-1765. Erratum: *Phys. Fluids A* **3**, 3128.

Jiménez, J., & Vasco, C. 1998 Approximate lateral boundary conditions for turbulent simulations. *Proceedings of the 1998 Summer Program*, Center for Turbulence Research, NASA Ames/Stanford Univ., 399-412.

Kravchenko, A., & Moin, P. 1998 B-spline methods and zonal grids for numerical simulations of turbulent flows. Dept. Mech. Eng. Rep. **TF-73**, Stanford Univ.

Le, H., Moin, P., & Kim, J. 1997 Direct numerical simulation of turbulent flow over a backward-facing step. *J. Fluid Mech.* **330,** 349-374.

Lilly, D. 1992 A proposed modification of the Germano subgrid-scale closure method. *Phys. Fluids A* **4**, 633-635.

Lund, T. S., Wu, X., & Squires, K. D. 1998 Generation of turbulent inflow data for spatially-developing boundary layer simulations. *J. Comp. Phys.* **140,** 233-258.

Na, Y., & Moin, P. 1998 Direct numerical simulation of a separated turbulent boundary layer. *J. Fluid Mech.* **374,** 379-405.

Nicoud, F., Winckelmans, G., Carati, D., Baggett, J., & Cabot, W. 1998 Boundary conditions for LES away from the wall. *Proceedings of the 1998 Summer Program*, Center for Turbulence Research, NASA Ames/Stanford Univ., 413-422.

Shur, M., Spalart, P. R., Strelets, M., & Travin, A. 1998 Detached-eddy simulation of an airfoil at high angle of attack. Preprint.

Smagorinksy, J. 1963 General circulation experiments with the primitive equations. I. The basic experiment. *Mon. Weather Rev.* **91,** 99-164.

Spalart, P. R. 1988 Direct numerical simulation of a turbulent boundary layer up to $Re_\theta = 1400$. *J. Fluid Mech.* **187,** 61-98.

Vasilyev, O. V., Lund, T. S., & Moin, P. 1998 A general class of commutative filters for LES in complex geometries. *J. Comp. Phys.* **146,** 82-104.

Vreman, B., Geurts, B., & Kuerten, H. 1994 On the formulation of the dynamic mixed subgrid-scale model. *Phys. Fluids* **6**, 4057-4059.

Zang., Y., Street, R. L., & Koseff, J. R. 1993 A dynamic mixed subgrid-scale model and its application to turbulent recirculating flows. *Phys. Fluids A* **5**, 3186-3196.